Inverted Equilibrium of a Vertically Driven Physical Pendulum

Woody Shew

Submitted to Dr. Don Jacobs

in partial fulfillment of Junior Independent Study

College of Wooster

4-24-97

Abstract: The suspension point of a physical pendulum with moment of inertia 2.72 g cm^2 was oscillated at frequencies ranging from 2.00 to 49.75 ± .005 Hz and amplitudes ranging from .23 to 1.33 ± .03 cm. The bounds of the resulting stability for the inverted equilibrium were examined theoretically and verified experimentally for the lower bound. The lower and upper bounds are given by the lines $\varepsilon = \sqrt{2}/\Omega$ and $\varepsilon = .45 + 1.799/\Omega^2$ respectively. End over end rotation, Hopf bifurcation, and the upper bound for the vertically down equilibrium were observed and analyzed on a qualitative level.

Introduction

A physical pendulum has two equilibrium position if the point of suspension or pivot point is held at a constant position. The vertically down position is a stable equilibrium while the vertically up or inverted equilibrium is clearly unstable. If the pendulum is released from any position other than precisely straight up, then the pendulum will fall and oscillate about the vertically down position with decreasing amplitude until it comes to rest.

If the pivot of the pendulum is not stationary, but instead is oscillated vertically, then the behavior of the pendulum changes dramatically. At certain frequencies and amplitudes of pivot oscillation, the inverted equilibrium of the pendulum becomes stable. This stabilization of the inverted equilibrium plays an important role in other physical systems such as quadrapole mass filters and various types of plasma containment. Accompanying pivot oscillation, there is also a upper boundary to the stability of the vertically down equilibrium with an oscillating pivot. End over end rotation becomes a very stable equilibrium motion. Perhaps the most bizarre behavior induced by the oscillating pivot is the existence of a state near the upper bound of the inverted equilibrium in which the pendulum oscillates back and forth between two positions on either side of the vertical position without amplitude decay. This state is called Hopf bifurcation.

This experiment uses a pendulum with moment of inertia 2.72 g cm^2 to examine thoroughly the inverted equilibrium. Primarily qualitative observations were made of the upper bound of the down equilibrium, end over end rotation, and Hopf bifurcation.

Theory

In researching the theory behind the equilibria of a physical pendulum, particularly the inverted equilibrium, I found several approaches to tackling the problem.[1,2,3,6] Two

approaches were particularly useful. The authors of the first, F. M. Phelps, III and J. H. Hunter, Jr., developed analytic solutions for several scenarios of driving forces on the pivot of a physical pendulum including the vertical oscillation of system that I have studied.[1,5] The second approach, developed by Henry P. Kalmus, is a very effective method for understanding and visualizing the phenomena of the inverted equilibrium of a pendulum on a utilitarian level.[2]

Equation of Motion

I'll begin with the general equation of motion of a nonlinear, inverted, physical pendulum. Consider the situation illustrated in Figure 1.

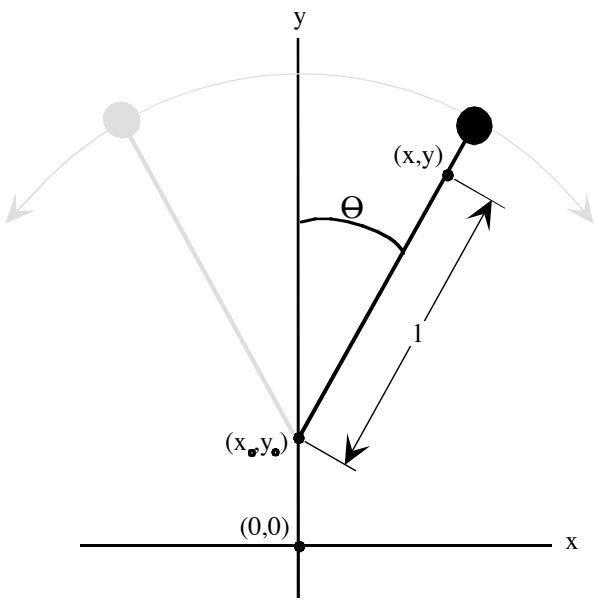

Figure 1. A pendulum with center of mass at (x,y) a distance l away from the pivot point (x_O,y_O) is free to rotate through the angle θ.

The only degree of freedom that this system has is rotation through the angle θ. Then Lagrange's equation in terms of θ is

$$\frac{d}{dt}\left(\frac{\partial T}{\partial \theta}\right) - \frac{\partial T}{\partial \theta} + \frac{\partial V}{\partial \theta} = 0\,, \qquad (1)$$

where T is kinetic energy, V is potential energy, and t is time. If the point of suspension or pivot point (x_O,y_O) of the pendulum is oscillated harmonically in the vertical directions, then

$$x_O = 0, \tag{2}$$

$$y_O = A\cos\omega t, \tag{3}$$

where ω and A are the frequency and amplitude of the pivot oscillations. The kinetic energy of the pendulum is then the sum of translational and rotation components of the velocity of the center of mass of the pendulum (x,y).

$$T = \frac{1}{2}m\dot{x}^2 + \frac{1}{2}m\dot{y}^2 + \frac{1}{2}I_0\dot{\theta}^2, \tag{4}$$

where m is the mass of the pendulum, I_O is the rotational inertia of the pendulum about the origin, and θ is the angular displacement from vertical as Figure 1 indicates. The potential energy of the system is just

$$V = mgy, \tag{5}$$

where g is acceleration due to gravity. In order to employ Lagrange's equation, I will express x and y in terms of θ.

$$x = l\sin\theta \tag{6}$$

$$y = A\cos\omega t + l\cos\theta \tag{7}$$

and differentiate to get

$$\dot{x}^2 = l^2(\cos^2\theta)\dot{\theta}^2 \tag{8}$$

$$\dot{y}^2 = A^2\omega^2\sin^2(\omega t) + 2Al\omega\sin(\omega t)\dot{\theta}\sin\theta + l^2(\sin^2\theta)\dot{\theta}^2 \tag{9}$$

On substituting eqs. (8) and (9) into (4) and (5) we get T and V in terms of θ and t.

$$T = \frac{1}{2}m\left[l^2\dot{\theta}^2 + A^2\omega^2\sin^2(\omega t) + 2Al\omega\sin(\omega t)\dot{\theta}\sin\theta\right] + \frac{1}{2}I_0\dot{\theta}^2 \tag{10}$$

$$V = mg(A\cos\omega t + l\cos\theta) \tag{11}$$

I_O can be expressed in terms of the rotational inertia I about the pivot point (x_O,y_O).

$$I = I_o + ml^2 \tag{12}$$

Substitute (12) into (10) and the kinetic energy becomes

$$T = \frac{1}{2}I\dot{\theta}^2 + \frac{1}{2}mA^2\omega^2\sin^2(\omega t) + Alm\omega\sin(\omega t)\dot{\theta}\sin\theta. \tag{13}$$

Now differentiate the kinetic and potential energies to use in Lagrange's equation.

$$\frac{\partial T}{\partial \dot{\theta}} = I\dot{\theta} + Alm\,\omega \sin(\omega t)\sin\theta \tag{14}$$

$$\frac{d}{dt}\left(\frac{\partial T}{\partial \dot{\theta}}\right) = I\ddot{\theta} + Alm\,\omega^2 \cos(\omega t)\sin\theta + Alm\,\omega \sin(\omega t)\dot{\theta}\cos\theta \tag{15}$$

$$\frac{\partial T}{\partial \theta} = Alm\,\omega \sin(\omega t)\dot{\theta}\cos\theta \tag{16}$$

$$\frac{\partial V}{\partial \theta} = -mgl\sin\theta \tag{17}$$

Substitute eqs. (15), (16), and (17) into eq. (1) and rearrange to find the equation of motion.

$$\ddot{\theta} + \left(\frac{Alm\,\omega^2 \cos(\omega t) - mgl}{I}\right)\sin\theta = 0 \tag{18}$$

For the inverted equilibrium of a pendulum the angle θ is generally small and $\sin\theta$ is approximately θ. Recall that $y_O = A\cos\omega t$ and $I = ml^2$ the equation of motion then can be written more simply as

$$\ddot{\theta} - \left(\frac{\ddot{y}_o + g}{l}\right)\theta = 0\,. \tag{19}$$

Until now I have neglected the fact that the motion of the pendulum is damped and energy is lost to friction at the pivot and to air resistance. For this experiment the energy lost to damping turns out to be small enough to be ignored. This is apparent if the solutions to eq. (19) are examined in the absence of a driving force (i.e. $\ddot{y}_o$=0) and with a angular velocity dependent damping term $2\beta\dot{\theta}$ included.

$$\ddot{\theta} + 2\beta\dot{\theta} - \left(\frac{g}{l}\right)\theta = 0 \tag{20}$$

This model assumes that as the velocity increases the energy lost to damping also increases. The solutions to eq. (20) look like

$$\theta(t) = e^{-\beta t}\left[A\exp\left(t\sqrt{\beta^2 - \omega_o^2}\right) + B\exp\left(-t\sqrt{\beta^2 - \omega_o^2}\right)\right] \tag{21}$$

where ω_o is the natural frequency of the pendulum and A and B are constants that depend upon the initial conditions. If the damping parameter β small enough, i.e. $\beta^2 << \omega_o^2$, then the damping of the pendulum's motion may be neglected. Two successive amplitudes of non-driven oscillation separated by one full period were measured experimentally. Assuming that the two amplitudes A_1 and A_2 fall on an exponentially decaying line through

all of the positive amplitude peaks from $0 > t > \infty$ as pictured in Figure 2, then they are related as

$$A_2 = A_1 e^{-\beta\tau} \tag{22}$$

where τ is the period of the oscillations.

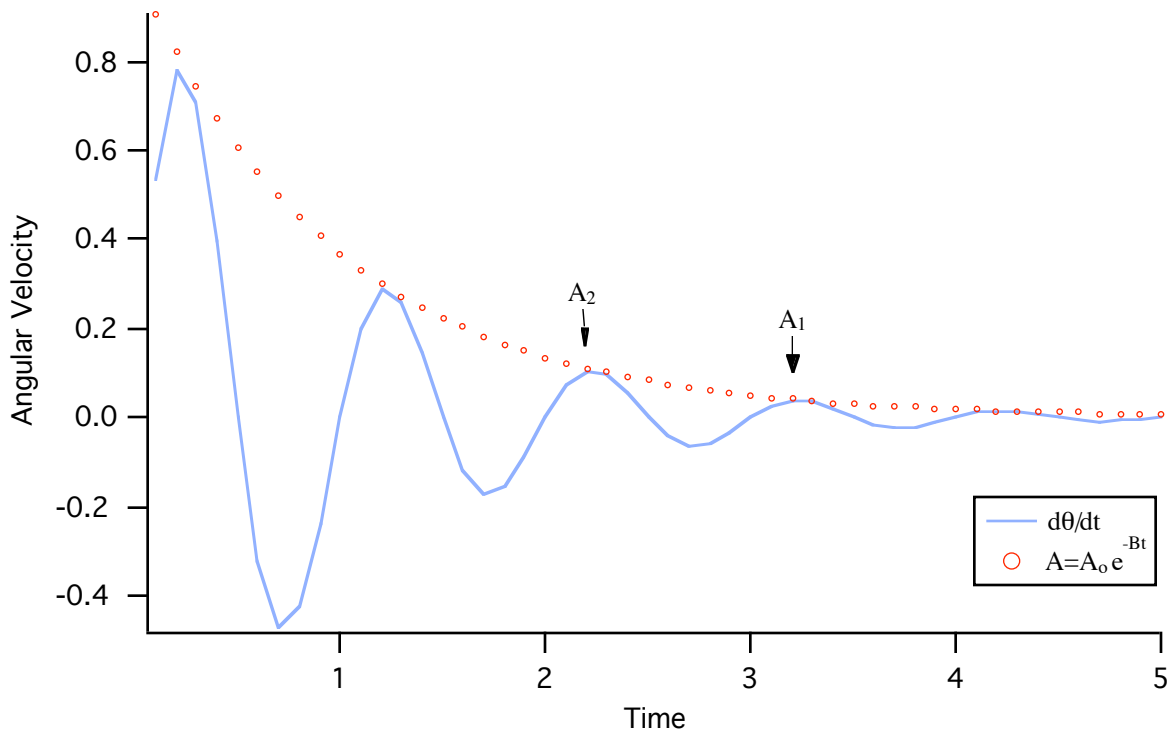

Figure 2. The amplitudes of successive non-driven oscillations decrease exponentially with time due to the damping of friction.

Substitute $\tau = \frac{2\pi}{\omega_o}$ into eq (22) to get

$$A_2 = A_1 e^{-2\pi\left(\frac{\beta}{\omega_o}\right)}. \tag{23}$$

This equation can be rearranged to

$$\frac{1}{2\pi}\ln\left(\frac{A_1}{A_2}\right) = \frac{\beta}{\omega_o}. \tag{24}$$

Using eq. (24), I calculated the ratio $\frac{\beta}{\omega_o}$ from the amplitudes that I measured A_1 and A_2. I found that the average for thirteen pairs of amplitudes was $\frac{\beta}{\omega_o}$=.345 with a standard deviation of .032. This implies $\beta = .345\,\omega_o$. For this value of β the inequality $\beta^2 << \omega_o^2$ is

true. Explicitly the inequality is $.119\omega_o^2 << \omega_o^2$ and therefore the damping is small enough to be ignored.

The Inverted Equilibrium

In order to understand how the inverted equilibrium works I will consider a slightly less complicated driving acceleration $\ddot{y}_o$. Consider $\ddot{y}_o$ = a applied in short bursts or impulses each of time τ in alternating directions of positive and negative $\hat{y}$ as shown in Figure 3. This sort of impulsive forcing yields a triangular displacement of the pendulum pivot as shown in Figure 4, which is similar to the actual sinusoidal displacement of the oscillator used in the experiment.

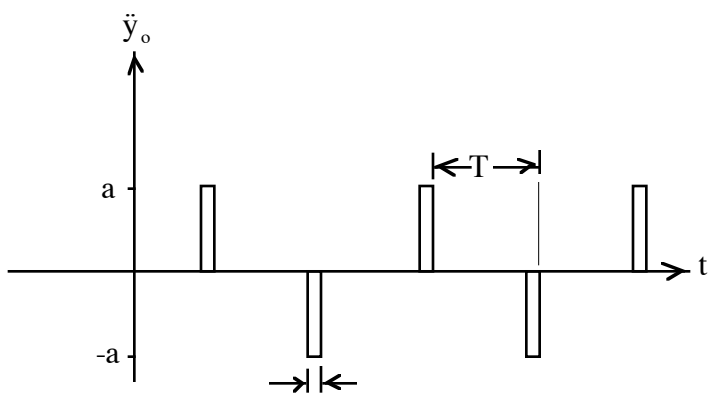

Figure 3. Acceleration of the pivot verses time.

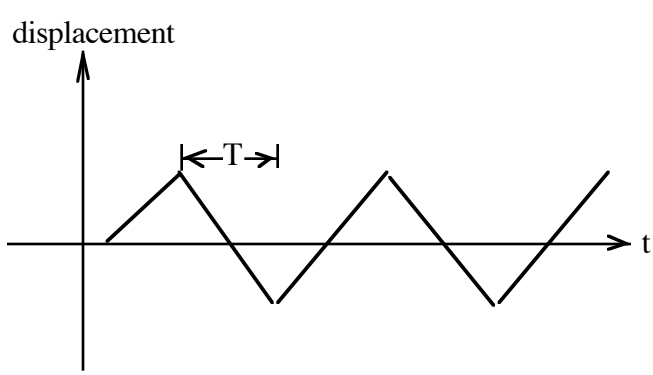

Figure 4. Displacement of the pivot verses time due to the acceleration illustrated in Figure 2.

Now rearrange eq. (18) with positive acceleration in the direction of g to obtain the expression

$$\ddot{\theta} = -\left(\frac{a+g}{l}\right)\sin\theta. \tag{25}$$

Since $\ddot{y}_o$ is applied for only a very short time τ, $\sin\theta$ stays practically constant during τ. Integrating both sides with respect to time then gives

$$\dot{\theta} = -\int_0^{\tau}\left(\frac{a+g}{l}\right)\sin\theta dt \tag{26}$$

$$\dot{\theta} = -\frac{(a+g)\sin\theta}{l}\tau \tag{27}$$

If we now imagine the pendulum in the absence of a gravitational field, then eq (27) becomes

$$\dot{\theta} = -Ka\sin\theta \tag{28}$$

where K is a constant equal to $\frac{\tau}{l}$. The angular velocity $\dot{\theta}$ is proportional to the sin of the angular displacement θ. Given an initial angular displacement and time step T we can now in increments equal to T predict the angular velocity and displacement for as long a time as we like. If, for example, at time zero θ is θ_o then

$$\dot{\theta}_o = \text{-}Ka\sin(\theta_o) \tag{29}$$

after the first impulse of acceleration downward. $\dot{\theta}_o$ is negative. This means that the pendulum is moving towards the vertical position after the first impulse. After a time T, on the order of 10 to 20 msec, the new angular position θ_1 will be

$$\theta_1 = \theta_o + \dot{\theta}_o T. \tag{30}$$

We have chosen T and a so that the pendulum does not rotate past vertical before the second impulse alters the pendulum again. So θ_1 is less than θ_o, but not yet negative, or past the vertical $\theta = 0$ position. The second impulse, directed up this time, will produce a new angular velocity

$$\dot{\theta}_1 = \dot{\theta}_o + \text{-}K(\text{-}a)\sin(\theta_1). \tag{31}$$

$\dot{\theta}_o$ is negative and -K(-a)sin(θ_1) is positive, but less than $\dot{\theta}_o$ because θ_1 is smaller than θ_o. Therefore $\dot{\theta}_1$ is also negative but less than $\dot{\theta}_o$. The pendulum is still rotating towards the

vertical position, but not so quickly now. Figure 5 shows the first few angular displacements as computed above.

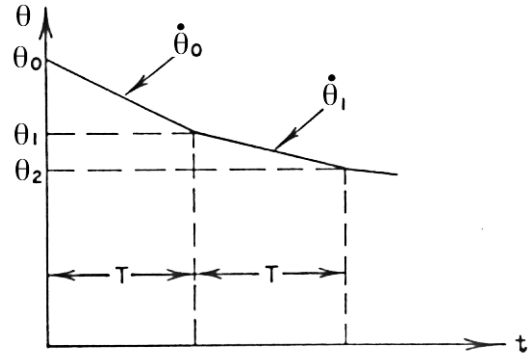

Figure 5. The decreasing slopes of the angular position verses time plot indicate a decreasing angular velocity as the pendulum approaches vertical.

Continuing this stepwise analysis of the position and velocity of the pendulum we would see that, after many driving cycles, the pendulum will oscillate about the vertical with a frequency much less that the frequency of the driving acceleration a. Figure 6 shows a nearly complete period of the pendulum's oscillation.

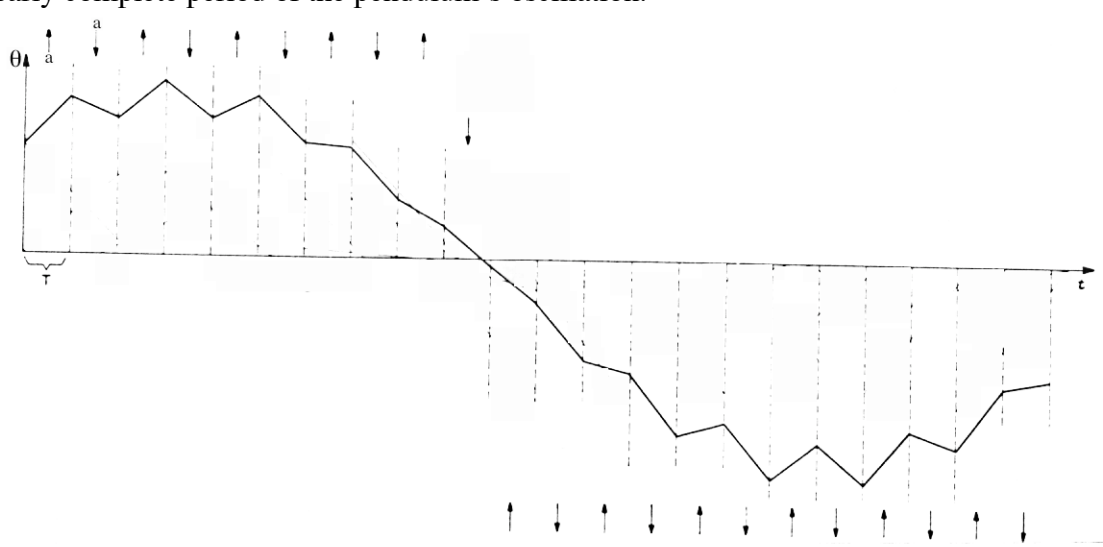

Figure 6. One cycle of the pendulum's oscillation about the vertical equilibrium while the pivot is oscillated vertically.

With damping due to friction, which was neglected in the stepwise analysis, the pendulum will oscillate about vertical with decreasing amplitude until it comes to rest straight up. If the pendulum is in a gravitational field, the straight lines for each time interval

in Figure 5 and Figure 6 become curved upward as gravity adds a continuous torque to the pendulum. With gravity our step by step analysis may have resulted in an increasing θ instead of decreasing. In other words if the periodic acceleration a is too weak, the inverted equilibrium will not be stable and the pendulum will fall to the vertically down position. The precise conditions for the stability of the inverted equilibrium are more complicated than can be demonstrated fully with the simple the stepwise analysis method.

Equation (18) can be rewritten as follows

$$\ddot{\theta} + \left(-\frac{mgl}{I} + \frac{Alm\omega^2}{I}\cos(\omega t) \right)\theta = 0 \tag{32}$$

where $\theta \approx \sin\theta$ because we're only looking at a small range of angles about the upright vertical position. Eq. (32) is a Mathieu equation of the general form

$$\frac{d^2u}{dz^2} + (A + 2B\cos 2z)u = 0 \tag{33}$$

which can be solved with as much accuracy as desired. I'll now introduce the reduced units $\Omega = \frac{\omega}{\omega_o}$ and $\varepsilon = \frac{A\omega_o^2}{g}$ where $\omega_o = \sqrt{\frac{mgl}{I}} = \sqrt{\frac{g}{l}}$. Ω and ε are the reduced unit equivalents of frequency and amplitude of the pivot oscillation. The constants A and B in eq. (33) can be written in terms of Ω and ε as follows

$$A = \frac{-4}{\Omega^2} \quad \text{and} \quad B = 2\varepsilon \tag{34}$$

The lower bound of stability for the inverted equilibrium is then given by the line

$$\varepsilon = \frac{\sqrt{2}}{\Omega} \tag{35}$$

in the ε-Ω plane. The upper bound for stability is given by

$$\varepsilon = 0.45 + \frac{1.799}{\Omega^2} \tag{36}$$

according to Phelps and Hunter[5,1] and Smith and Blackburn[3,4]. Figure 7 shows the two boundary lines plotted in the ε-Ω plane.

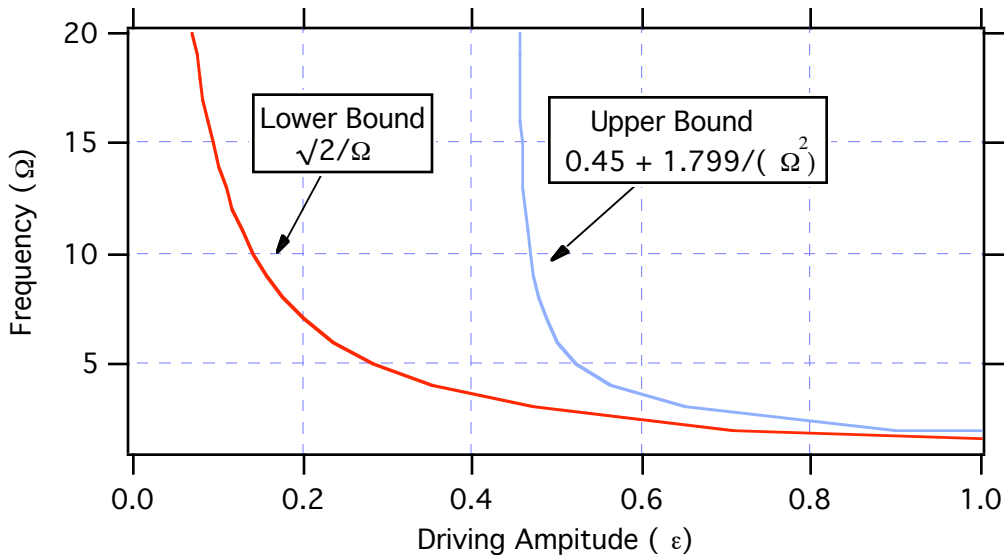

Figure 7. The region in between the two lines in the above plot represents the collection possible parameter values that produce a stable inverted equilibrium.

Setup & Procedure

The pendulum used in this experiment consists of a 2.1 ± .05 cm nylon screw attached at one end to the shaft of a Minimotor SA CH 6982AGNO so that it's motion sweeps out a circle of radius equal to the length of the screw in a plane perpendicular to the motor shaft as shown in Figure 8. Threaded to the other end of the nylon screw there is a steel nut and a steel washer of combined mass 1.311 ± .0005 g. The center of mass of the nut and washer is a distance 1.4 ± .1 cm from the axis of rotation. An 0.6 ± .05 cm long aluminum axle of radius .33 ± .025 cm is epoxied to the motor shaft parallel to the axis of rotation. A hole was drilled in the aluminum axle perpendicular to the axis of rotation into which the nylon screw was epoxied.

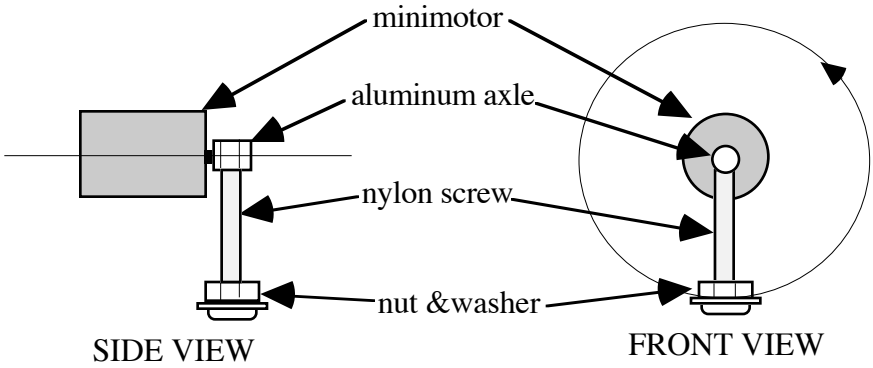

Figure 8. The pivot of the pendulum is the shaft of a minimotor. The arm of the pendulum consists of a nylon screw with a steel nut and washer at one end.

The moment of inertia of the pendulum (i.e. the combined axle, screw, nut, and washer) about the axis of rotation through the motor shaft is 2.72 g cm^2.

The motor is attached with a pipe clamp to a support brace made from .05 cm thick copper sheet metal as illustrated in Figure 9. In addition to holding the motor, the support brace also secured the wires from the motor leads to the whole device so that stress on the lead connections is minimized when the motor is oscillated. Before the wires were secured they had a tendency to break of at the soldered lead connections. The base of the support brace is fastened to a banana plug that fits into the shaft of a PASCO Mechanical Vibrator Model SF-9324. The vibrator was driven by a PASCO Digital Function Generator-Amplifier Model PI-9587 as shown in Figure 10.

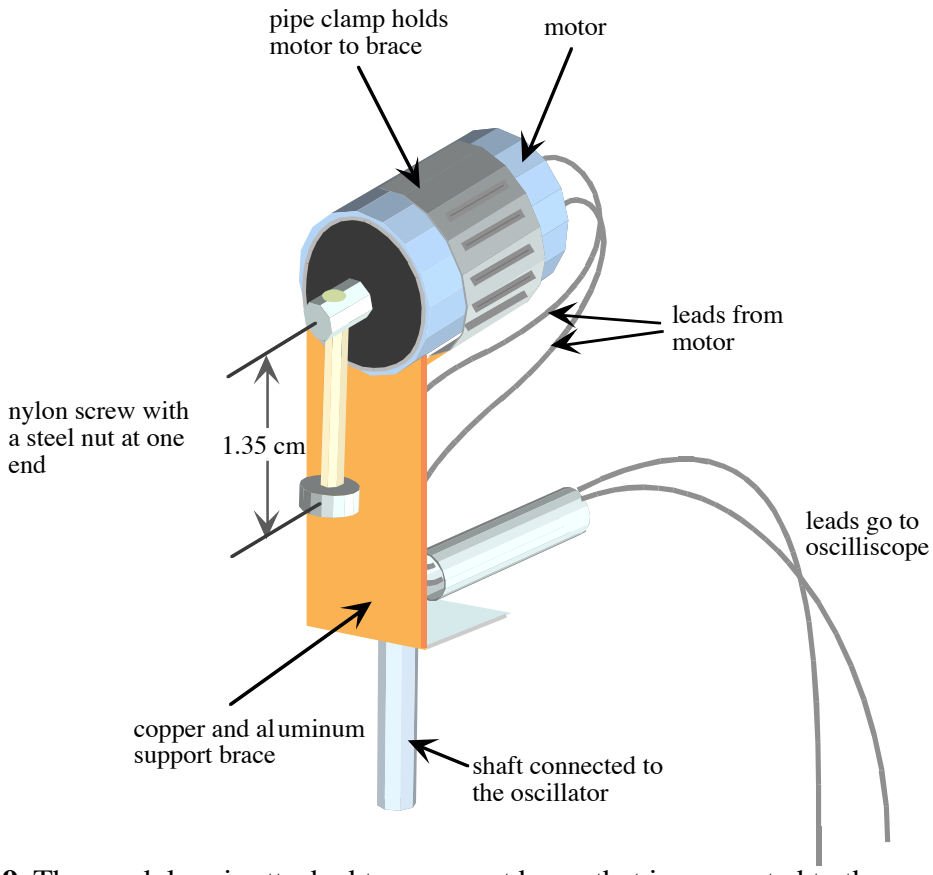

Figure 9. The pendulum is attached to a support brace that is connected to the mechanical vibrator.

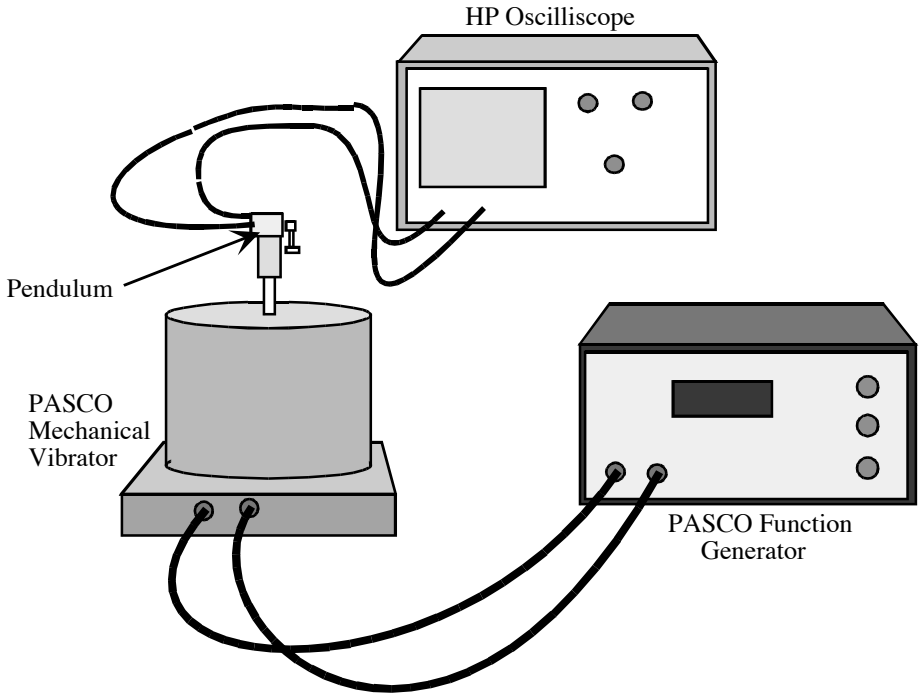

Figure 10. The pendulum is oscillated by the vibrator which is driven by the function generator.

A motor was used for the pivot of the pendulum so that any motion of the pendulum could be observed as a voltage across the leads of the motor read by a Hewlett Packard 54600A 100 MHz 2 Channel Oscilloscope. It turns out that this idea is not entirely useful. When the whole apparatus was vibrated at frequencies anywhere above about 10 Hz the voltage from the motor was too noisy to obtain accurate information about the pendulum's motion. Despite failure of measuring the driven pendulum's motion, the natural frequency of the pendulum was successfully obtained using the motor voltage. With the vibrator off, the pendulum was give an initial angular displacement of about $\pi/2$ and then released. The oscilloscope displayed the resulting sinusoidal voltage with the same frequency as the oscillation of the pendulum. Positioning the cursors on the oscilloscope display at the peaks of the oscillating voltage, I measured the natural frequency of the pendulum motion. I repeated this process eighteen times and found the average natural frequency ω_o to be 25.9 Hz with a standard deviation of 1.75 Hz.. I took measurements only from the last few oscillations each time so that the angle through which the pendulum swung was small enough to use the small angle approximation with later calculations. The corresponding theoretical value $\omega_o = \sqrt{\frac{g}{l}}$, where l is the distance from the axis of rotation to the center of mass of the pendulum, was calculated to be 25.7 Hz.

In order to characterize the bounds of the inverted equilibrium of the pendulum, I compared the reduced unit quantities $\Omega = \frac{\omega}{\omega_o}$ and $\varepsilon = \frac{A\omega_o^2}{g}$ introduced in the theory. Substituting g = 981 cm/s^2 and the experimentally determined value $\omega_o = 25.9 \pm 1.75$ Hz into these two expressions gave me functions dependent only upon the linear driving frequency f and amplitude A of the mechanical vibrator.

$$\Omega(f) = .242f \quad \text{and} \quad \varepsilon(A) = .684A \tag{37}$$

The linear frequency f is displayed on the function generator and the amplitude was measured by sticking a piece of tape to the shaft of the vibrator and holding a pen to the tape while it vibrated. Half the length of the mark left on the tape is the driving amplitude A.

Though the function generator does have a amplitude control knob, the maximum amplitude is dependent upon the frequency. In Figure 11 is a plot of maximum ε values for Ω varying from 0 to 12. These values were collected by turning the amplitude control knob to the maximum position and then measuring the amplitude with the pen-and- tape method for a range of frequencies that give the range of Ω plotted in Figure 11.

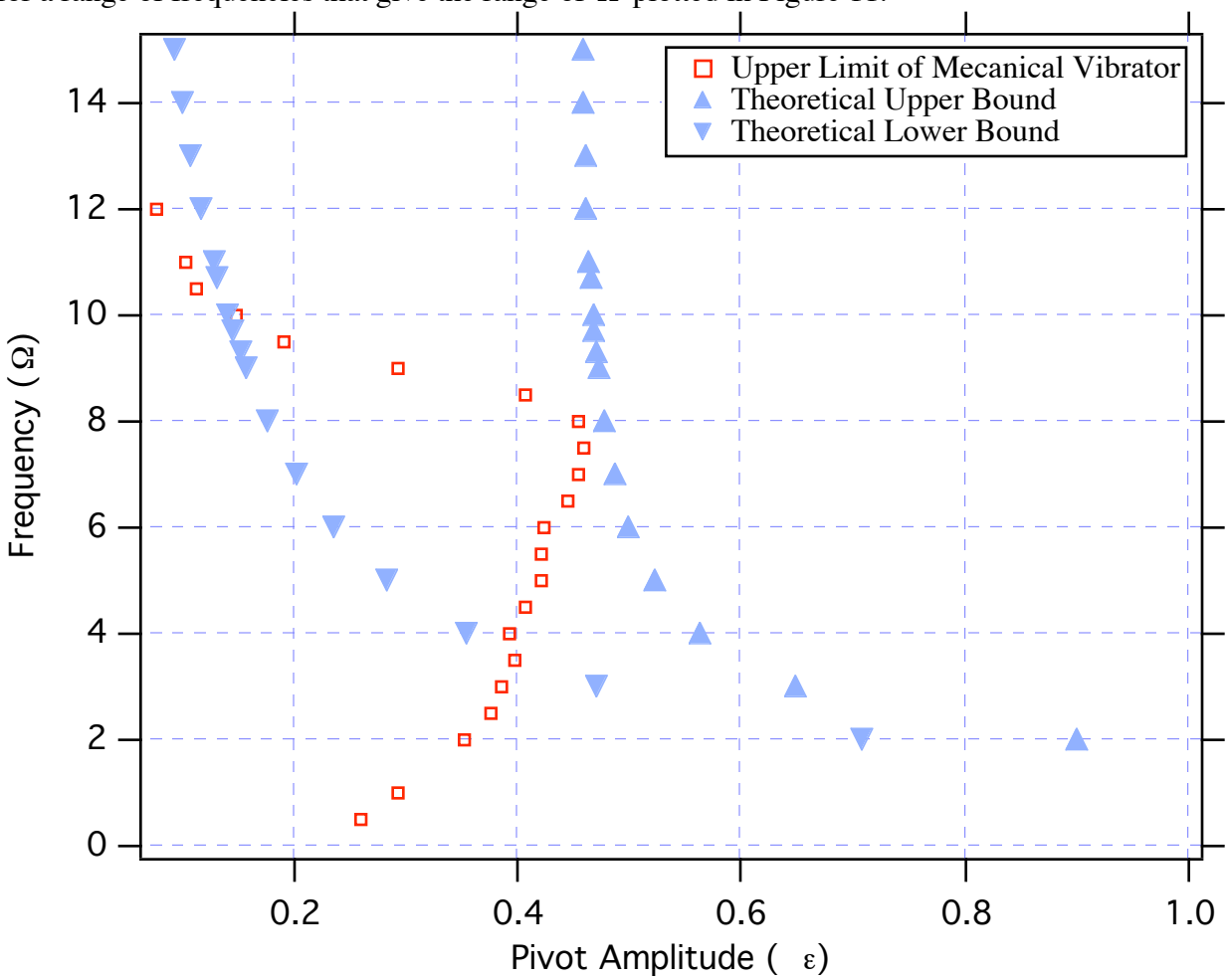

Figure 11. The shaded region is the possible values of ε and Ω for which the pendulum can exist in the stable inverted equilibrium.

Only ε and Ω values that fall to the left of the Upper Limit of Mechanical Vibrator can be achieved with this setup. The shaded region represents the collection of ε and Ω values for which the pendulum of this experiment can be in the stable inverted equilibrium.

Data & Analysis

It is apparent in Figure 11 that my setup is capable only of revealing part of the lower bound of the inverted equilibrium. The method used to make observations of this

boundary was similar to that used to produce the data shown in Figure 11. I set and recorded the frequency signal from the function generator constant and turned the amplitude to a position that permitted stability in the inverted equilibrium. Then I reduced the amplitude slowly, careful not to decrease past the lower bound, until the pendulum fell out of equilibrium. I then measured the amplitude of the vibrator via the pen-and-tape method described above. From these recorded amplitude and frequency values, I used eqs. (37) to calculate ε and Ω. In Figure 12 is the first data that I collected.

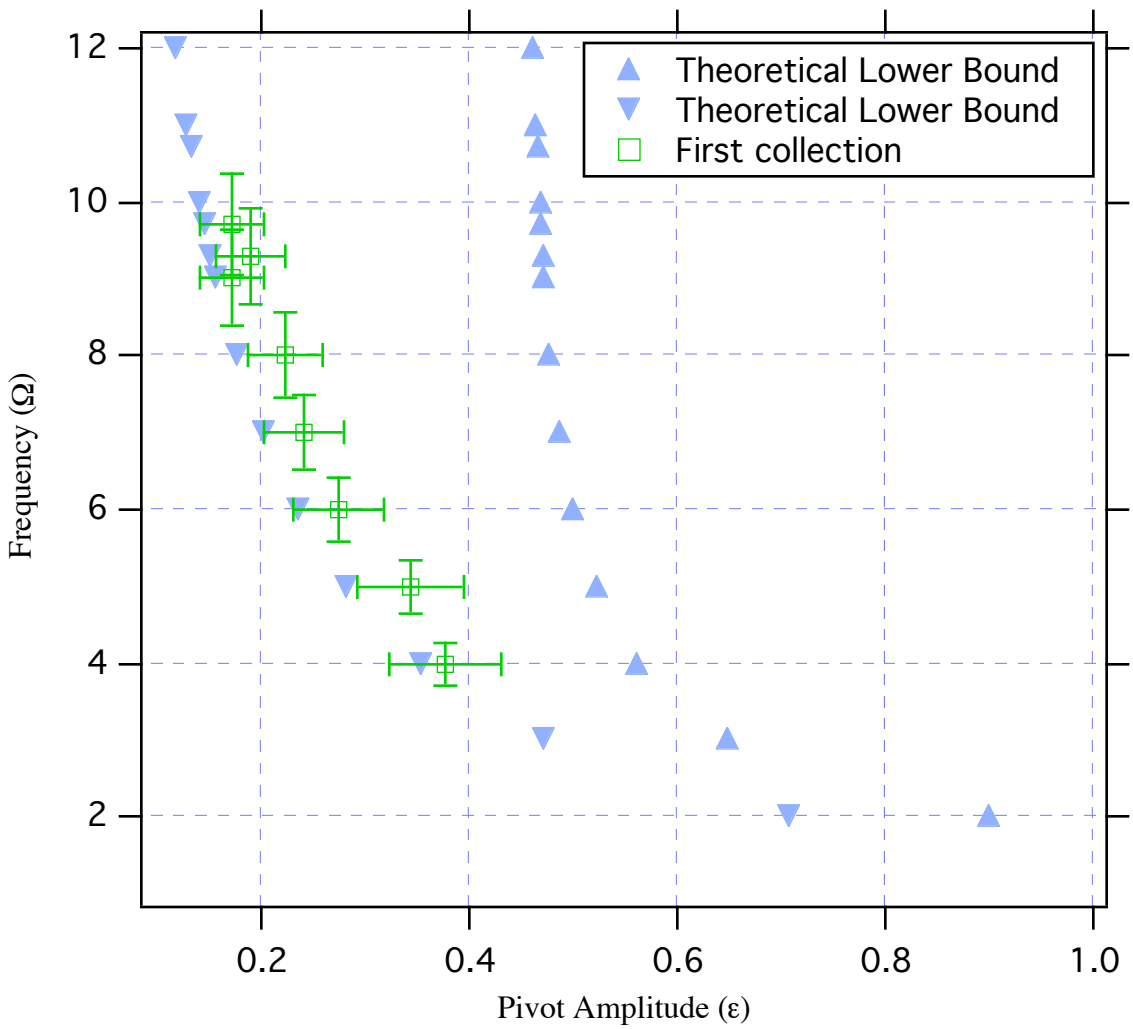

Figure 12. This is a plot of the collected values of lower bound of the inverted equilibrium.

The uncertainty indicated by the error bars in Figure 12 are due to uncertainty in measurement of amplitude, frequency, and moment of inertia of the pendulum. The uncertainty in Ω was calculated with the formula

$$\Delta\Omega = \sqrt{\left(\frac{\partial\Omega}{\partial\omega_o}\Delta\omega_o\right)^2 + \left(\frac{\partial\Omega}{\partial\omega}\Delta\omega\right)^2} \tag{38}$$

where

$$\frac{\partial\Omega}{\partial\omega_o} = -\frac{\omega}{\omega_o^2}, \quad \frac{\partial\Omega}{\partial\omega} = \frac{1}{\omega_o}, \quad \Delta\omega_o = 1.75 \text{ cm, and } \Delta\omega = .005 \text{ Hz.} \tag{39}$$

Now substitute eqs. (39) into eq. (38) to get the equation

$$\Delta\Omega = \sqrt{\left(-1.75\frac{\omega}{\omega_o^2}\right)^2 + \left(\frac{.005}{\omega_o}\right)^2} \tag{40}$$

The uncertainty in ε was calculated with the same method.

$$\Delta\varepsilon = \sqrt{\left(\frac{\partial\varepsilon}{\partial A}\Delta A\right)^2 + \left(\frac{\partial\varepsilon}{\partial\omega_o}\Delta\omega_o\right)^2} \tag{41}$$

where

$$\frac{\partial\varepsilon}{\partial A} = \frac{\omega_o^2}{g}, \quad \frac{\partial\varepsilon}{\partial\omega_o} = \frac{2A\omega_o}{g}, \quad \Delta A = .03 \text{ cm, and } \Delta\omega_o = 1.75 \text{ cm.}$$

Then

$$\Delta\varepsilon = \sqrt{\left(.03\frac{\omega_o^2}{g}\right)^2 + \left(3.5\frac{A\omega_o}{g}\right)^2}\,. \tag{42}$$

Possible error due to construction imperfections is not incorporated into these uncertainty formulas. The aluminum axle was probably not perfectly centered on the motor shaft. This and perhaps other flaws in construction may explain the apparent shift of all of the data slightly to the right of the predicted values.

The second collection of data is displayed in Figure 13.

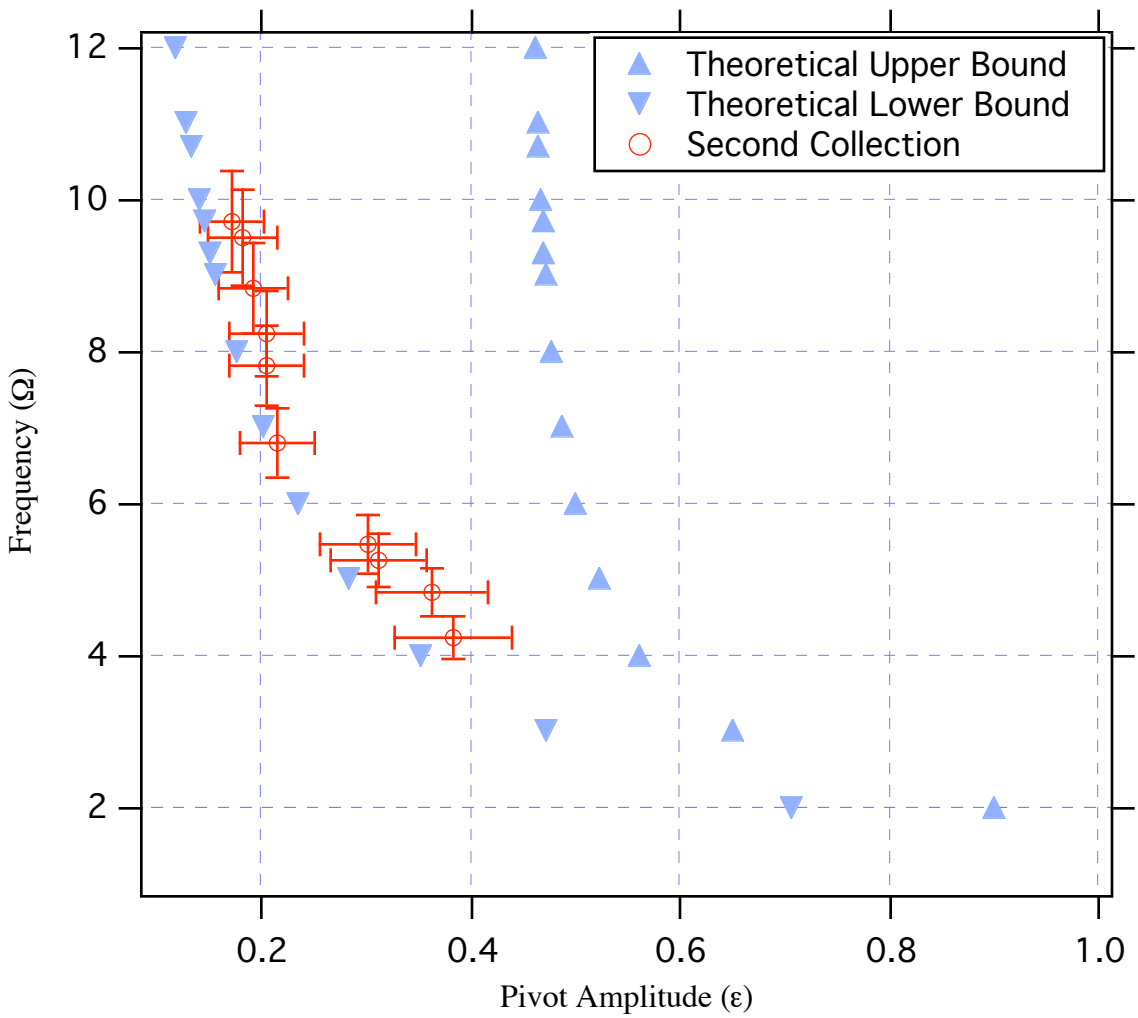

Figure 13. The second collection of data also fits the theoretical lower bound well.

This plot agrees very well with the first collection. The theoretical lower bound of the equilibrium falls within the uncertainty bars for nearly every point of both sets of data.

In addition to the inverted equilibrium, other stable equilibria were observed though not treated with as much depth theoretically. First, when I was measuring the upper limit of the vibrator, I noticed that at Ω near 7.9 the vertically down position of the pendulum did not behave as I had expected. Instead it began oscillating wildly back and forth sometimes evolving into a state of end over end rotation. Blackburn and Smith[4,3] have predicted and measured an upper bound to the stability of the vertically down state along the line $.45 - 1.799/\Omega^2$ in the ε - Ω plane. It turns out that the strange behavior that I noticed around Ω = 7.9 is where the line describing the vibrator's upper limit intersects Blackburn and Smiths

theoretical upper bound. I collected the few data points shown in Figure 14 that also displayed the erratic behavior just described. Using a similar method as with the inverted equilibrium data, I increased the amplitude of the vibrator at a set frequency until the unstable behavior showed itself. The resulting data matches the theoretical upper bound of the vertically down equilibrium.

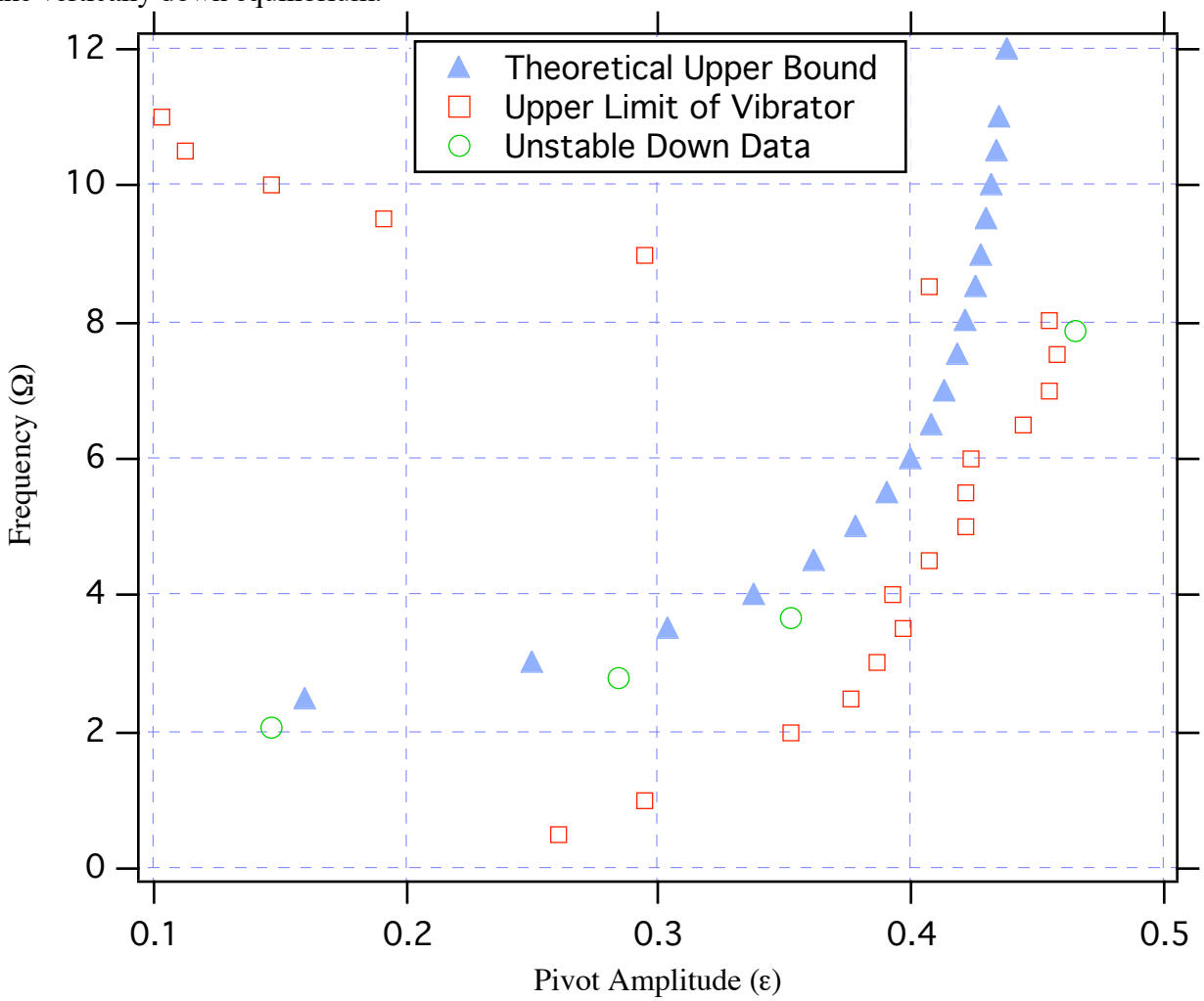

Figure 14. Erratic, unstable behavior of the vertically down equilibrium was observed at the points marked with circles.

Another stable state the nonlinear pendulum can occupy is end over end rotation. From purely qualitative observation, I think that this is stable for the widest range of ε and Ω values. I observed stability for all values except for very small amplitudes (ε on the order of .05 to .1) and very high frequencies (Ω on the order of 10) which are accompanied by very small amplitudes.

A final and most exotic stable state, called Hopf bifurcation, was also observed on a qualitative level. Hopf bifurcation is described by Blackburn and Smith as a *flutter mode* where the pendulum oscillates about the inverted vertical position at a frequency equal to half that of the drive frequency. I was able to put the pendulum into this state at frequencies around $\Omega = 6.7 - 8.5$ with the amplitude knob at maximum position. Using a PASCO Model SF 9211 Stroboscope driven at the same frequency as the vibrator, I was able to observe the characteristic half-drive frequency of the motion. If the Hopf motion has half the frequency of the stroboscope, then the stroboscope will flash twice per period of the Hopf motion and illuminate only the two extreme ends of the motion. This is the phenomenon that I observed. The pendulum exhibits Hopf bifurcation only when released from a particular initial angular displacement for ε and Ω values near the upper bound for stability of the inverted equilibrium. Unfortunately, observation of the upper bound of the inverted equilibrium is for the most part beyond the capabilities of the setup that I used.

Conclusions

In the experiment presented in this paper, a physical pendulum with a vertically oscillating pivot point was observed in several stable equilibria. Specifically, the upper and lower bounds of the inverted equilibrium were theoretically determined to be the lines $\varepsilon = .45 + 1.799/\Omega^2$ and $\varepsilon = \sqrt{2}/\Omega$ respectively. The lower bound was confirmed experimentally for a range of $\Omega \approx 4$ to $\Omega \approx 10$. The upper bound of the vertically down equilibrium was observed experimentally and shown to match a theoretical upper bound $\varepsilon = .45 - 1.799/\Omega^2$. Also observed were a stable end over end rotation for a broad range of frequencies and a state called Hopf bifurcation near the upper bound of the inverted equilibrium.

More conclusive data could be collected for the boundaries of the three states, vertically down, end over end rotation, and Hopf bifurcation and for the upper bound of the inverted equilibrium. With the setup used in this experiment the upper bound of the inverted equilibrium and much of the Hopf bifurcation was not attainable. A possible

remedy for these problematic limitations may be a pendulum with an adjustable center of mass (e.g. a long threaded pendulum arm with a mass that could be screwed on to the desired distance from the axis of rotation). By increasing distance of the center of mass from the axis of rotation, greater values of ε could be observed, as ε is inversely proportional to the natural frequency and the natural frequency is inversely proportional to the distance to the center of mass.

Other forms this experiment could take in the future could include the equilibria of a compound inverted pendulum. There is also potential for study of chaotic behavior at small driving frequencies. The simple pendulum has been a system under the scrutiny of physics for ages. Despite centuries of examination the simple pendulum continues to hold its place in contemporary mechanics and nonlinear dynamics[3].

Annotated Bibliography

1 F. M. Phelps, III and J. H. Hunter, Jr., "An Analytical Solution of the Inverted Pendulum," American Journal of Physics **33**, 285-295 (1965).

This is a rigorous mathematical approach to several scenarios of pivot driving forces including the vertical oscillation of this experiment. This was useful for deriving an equation of motion using Lagrange's equation.

2 Henry P. Kalmus, "The Inverted Pendulum," American Journal of Physics **38**, 874-878 (1970).

Kalmus used a step by step analysis of the motion of a inverted pendulum with an impulsive, vertically oscillating pivot acceleration. This was very helpful for developing an understanding of the reason the inverted equilibrium is stable.

3 James A. Blackburn, H. J. T. Smith, N. Gronbech-Jensen, "Stability and Hopf Bifurcations in an Inverted Pendulum," American Journal of Physics **60**, 903-907 (1992).

The authors used numerical simulations to investigate the inverted pendulum. They examined associated basins of attraction and regions of Hopf bifurcation. This article was helpful for determining the characteristics of Hopf bifurcations and regions of stability for other equilibria.

4 H. J. T. Smith and J. A. Blackburn, "Experimental Study of an Inverted Pendulum", American Journal of Physics **60**, 909-911 (1992).

This article was very useful for determining initial parameter values for the construction of the pendulum. I also used the method used by Smith and Blackburn to analyze my data.

5 F. M. Phelp, III and J. H. Hunter, Jr., "Reply to Joshi's Comments on a Damping Term in the Equations of Motion of the Inverted Pendulum," American Journal of Physics **34**, 533-535 (1966).

This article was useful for determining the bounds of the inverted equilibrium.

6 Leon Blitzer, "Inverted Pendulum", American Journal of Physics **33**, 1076-1077 (1965).

A Newtonian approach to an equation of motion for the inverted pendulum.

7 Douglass J. Ness, "Small Oscillations of a Stabilized, Inverted Pendulum," American Journal of Physics **35**, 964-967 (1967).

This pendulum used by Ness did not have a traditional pivot, but instead had a mass attached to a flexible piece of metal that acted as a hinge. This was not directly applicable to the system that I studied.

8 D. W. Jordan and P. Smith, *Nonlinear Ordinary Differential Equations* , Second Edition (Oxford University Press, New York, 1987), pp. 245-257.

This is a mathematical text useful for understanding the solutions of the equations of motion.

9 Jerry B. Marion and Stephen T. Thornton, *Classical Dynamics of Particles and Systems,* Fourth Edition (Harcourt Brace College Publishers, New York, 1995) pp. 116-119.

This text was useful for determining whether or not the damping of the studied pendulum was negligible.

10 John L. Synge and Byron A. Griffith, *Priciples of Mechanics*, Second Edition (McGraw-Hill Book Company, Inc., New York, 1949) pp. 189-193.

I used this calculate the moment of inertia of the pendulum. It was also helpful for developing a basic understanding of the motion of a physical pendulum.

11 K. E. Bullen, *An Introduction to the Theory of Mechanics*, Eighth Edition (Cambridge University Press, Cambridge, 1971) pg 231.

This text was also useful for beginning a theoretical treatment of the motion of a rigid body pendulum.